

RSC Advances



This is an *Accepted Manuscript*, which has been through the Royal Society of Chemistry peer review process and has been accepted for publication.

Accepted Manuscripts are published online shortly after acceptance, before technical editing, formatting and proof reading. Using this free service, authors can make their results available to the community, in citable form, before we publish the edited article. This *Accepted Manuscript* will be replaced by the edited, formatted and paginated article as soon as this is available.

You can find more information about *Accepted Manuscripts* in the [Information for Authors](#).

Please note that technical editing may introduce minor changes to the text and/or graphics, which may alter content. The journal's standard [Terms & Conditions](#) and the [Ethical guidelines](#) still apply. In no event shall the Royal Society of Chemistry be held responsible for any errors or omissions in this *Accepted Manuscript* or any consequences arising from the use of any information it contains.

Synthesis and physical properties of new layered silicates based on ionic liquids: Improvement of thermal stability, mechanical behaviour and water permeability of PBAT nanocomposites

Sébastien Livi^{a*}, Gabriela Sar^a, Valeria Bugatti^c, Eliane Espuche^b, Jannick Duchet-Rumeau^a

^a *Université de Lyon, F-69003, Lyon, France; INSA Lyon, F-69621, Villeurbanne, France; CNRS, UMR 5223, Ingénierie des Matériaux Polymères.*

^b *Université de Lyon, F-69003, Lyon, France; Université Lyon 1, F-69622, Villeurbanne, France; CNRS, UMR 5223, Ingénierie des Matériaux Polymères.*

^c *Department of Industrial Engineering, University of Salerno, Via Ponte Don Melillo 1, 84084-Fisciano (SA), Italy*

Abstract

Ionic liquids based on tetraalkylphosphonium and dialkyl imidazolium cations with long alkyl chains have been investigated as new surfactant agents for cationic exchange of lamellar silicates. The effect of the chemical nature of the ionic liquids on the thermal stability and on the surface energies of phosphonium- (MMT-201) and imidazolium- (MMT-I) treated montmorillonites have been studied by thermogravimetric analysis (TGA) and sessile drop method. Poly(butylene adipate-co-terephthalate) (PBAT) nanocomposites filled with a low amount of these modified-montmorillonites (2, 5 wt %) have been processed by melt mixing using a twin screw extruder. The mechanical, thermal, water and gas barrier properties of the

corresponding nanocomposites as well as the distribution of the clay layers in PBAT matrix were determined.

Keywords: *Ionic liquids, Poly(butylene adipate-co-terephthalate), Biopolymer, Nanocomposites.*

1 Introduction

For several years, many efforts of academic and industrial research have been made to develop an ecofriendly way to prepare high performance polymeric materials for application in food packaging or in tissue engineering [1-3]. For these reasons, many biodegradable polymers of natural or synthetic origin such as polylactide (PLA), poly(3-caprolactone) (PCL), polyglycolide (PGA), poly(butylene adipate-co-terephthalate) (PBAT) have been extensively investigated [4-7]. More recently, due to their biodegradability and their good final properties, aliphatic-aromatic copolyesters such as PBAT synthesized from 1,4-butanediol, adipic acid and terephthalic acid are the target of the research. In fact, the higher elongation at break of poly(butylene adipate-co-terephthalate) makes it an excellent candidate for the production of compostable and biodegradable films [8]. Nevertheless, the use of nanoparticles is required to improve the mechanical properties as well as the water and gas barrier properties [9]. Due to their excellent mechanical and optical properties as well as their high surface area, layered silicates, especially montmorillonite (MMT) have been investigated in the literature to enhance the thermal, mechanical, rheological and barrier properties of PBAT matrix [10-11]. However, the use of ammonium salts which begins to degrade from 180 °C could compromise the final properties of the PBAT nanocomposites [12].

For this reason, ionic liquids (ILs) which are organic salts with low melting temperature (<100°C) represent an alternative to conventional ammonium salts. In fact, their unique properties such as an excellent thermal and chemical stability, their low vapour pressure and their no flammability make ionic liquids increasingly used in the polymers as

surfactant of layered silicates [13-15], plasticizers [16], lubricants [17], building blocks [18] or new additives of epoxy prepolymer [19, 20].

In this work, thermally stable imidazolium- and phosphonium-modified montmorillonites were prepared to improve the final properties of PBAT nanocomposites. Thus, the influence of a small amount (2 and 5 wt%) of organically treated MMT were investigated on the mechanical properties and the water/gas barrier properties. In addition, synergy between the ionic liquids used as additives and the ILs-treated montmorillonites was also investigated on the behavior of these nanocomposites.

2 Experimental

2.1 Materials

A sodic montmorillonite denoted Nanofil 757 (MMT- Na^+) was selected as pristine clay and was provided by Süd Chemie Co (Germany). Its cation exchange capacity (CEC) is 95meq/100g and is described by the following formula $\text{Na}_{0.65}[\text{Al,Fe}]_4\text{Si}_8\text{O}_{20}(\text{OH})_4$. All chemicals necessary to the synthesis of imidazolium salt, *i.e.* imidazole (99.5%), 1-iodooctadecane (95%) and solvents (acetonitrile, methanol and pentanol) were supplied by Aldrich and used as received. The Poly(butylene adipate-co-terephthalate) used in this work, named PBAT, was supplied by BASF (Germany) under the trade name of Ecoflex. The ionic liquid denoted IL201 based on tributyltetradecylphosphonium cation associated with dodecylbenzenesulfonate anion was provided by Cytec Industries Inc (Canada).

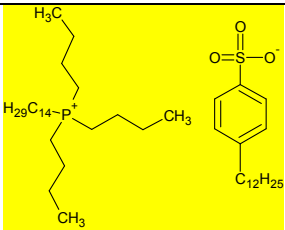
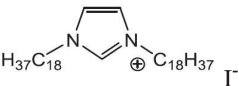
2.2. Synthesis of imidazolium ionic liquid

The synthesis of N-octadecyl-N'-octadecyl imidazolium salt denoted IL-I was already reported in a previous work [21]. The synthesis of salts was checked by ^1H NMR and ^{13}C NMR spectroscopy collected on a Bruker AC 250 (250 MHz) spectrometer.

2.3. Organic modification of montmorillonite

Based on the cation exchange capacity (CEC = 95 meq/100 g) of the montmorillonite *Nanofil* 757 [22], 2 CEC of surfactant was firstly dissolved in 450 mL of THF/deionized water (2:1). Then, the montmorillonite was added slowly in the solution at 50 °C. This dispersion was mixed and stirred vigorously for 24 h, followed by filtration and three washing with deionized water until no halide ions were detected using an aqueous silver nitrate (AgNO_3) solution. Finally, the treated-montmorillonite was dried under vacuum overnight at 80 °C. Abbreviations used for ionic liquids and to design the different montmorillonites are presented in Table 1.

Table 1
Montmorillonites organically modified by different ionic liquids.

Ionic liquid	Chemical structure of the surfactant agent	Designation
IL201		MMT-201
IL-I		MMT-I

2.2 Processing and instrumental characterization of PBAT/OMMT nanocomposites

Nanocomposites based on PBAT/organically modified montmorillonites (2-5 % by weight) were prepared under nitrogen atmosphere using a 15 g-capacity DSM micro-extruder (Midi 2000 Heerlen, The Netherlands) with co-rotating screws. The mixture was sheared under nitrogen atmosphere for about 3 min with a 100 rpm speed at 160 °C and injected in a 10 cm³ mould at 40 °C to obtain dumbbell-shaped specimens. Formulations of PBAT/MMT-I, PBAT/MMT-201, PBAT/MMT-201 + IL 201, PBAT/MMT-I + IL-I were also made following the same procedure mentioned above, where the ionic liquid was added additionally within the nanocomposites.

Thermogravimetric analysis (TGA) of ionic liquids, clays (untreated and organically modified) and nanocomposites were performed on a Q500 thermogravimetric analyser (TA instruments). The samples were heated from room temperature to 600 °C at a rate of 20 K.min⁻¹ under nitrogen flow.

DSC measurements (DSC) of ionic liquids and nanocomposites were performed on a Q20 (TA instruments) from – 60 °C to 180 °C. The samples were kept for 1 min at 180 °C to erase the thermal history before being heated or cooled at a rate of 10 K.min⁻¹ under nitrogen flow of 50 mL.min⁻¹. The crystallinity was calculated with the heat of fusion for PBAT of 114 J/g [23].

Surface energy of modified MMTs was determined with the sessile drop method using a GBX goniometer. From contact angle measurements performed with water and diiodomethane as probe liquids on discs obtained from anionic clay powders by pressing,

polar and dispersive components of surface energy were determined by using Owens-Wendt theory [24].

Wide-angle X-ray diffraction spectra (WAXD) were collected on a Bruker D8 Advance X-ray diffractometer at the H. Longchambon diffractometry center. A bent quartz monochromator was used to select the Cu K α 1 radiation ($\lambda = 0.15406$ nm) and run under operating conditions of 45 mA and 33 kV in Bragg–Brentano geometry. The angle range scanned is 1–10° 2θ for the modified clays and for the nanocomposite materials.

Transmission electron microscopy (TEM) was carried out at the Center of Microstructures (University of Lyon) on a Philips CM 120 field emission scanning electron microscope with an accelerating voltage of 80 kV. The samples were cut using an ultramicrotome equipped with a diamond knife, to obtain 60-nm-thick ultrathin sections. Then, the sections were set on copper grids.

Uniaxial Tensile Tests were carried out on a MTS 2/M electromechanical testing system at 22 \pm 1 °C and 50 \pm 5% relative humidity at crosshead speed of 50 mm.min⁻¹.

Water Vapor Sorption experiments were performed using a conventional McBain spring balance system, which consists of a glass water-jacketed chamber serviced by a high vacuum line for sample degassing and permeant removal. Inside, the chamber samples were suspended from a helical quartz spring supplied by Ruska Industries, Inc. (Houston, TX) and had a spring constant of 1.52544 cm/mg. The temperature was controlled to 30 \pm 0.1 °C by a constant temperature water bath. Sorption was measured as a function of the relative pressure, $a=P/P_0$, where P is the actual pressure (in mmHg) of the experiment, and P₀ the saturation

pressure at 30°C for water (32 mmHg) during 24 h. The samples were exposed to the penetrant at fixed pressures ($a=0.53$), and the spring position was recorded as a function of time using a cathetometer. Data averaged on three samples. Diffusion coefficients and equilibrium mass uptake were extracted from these kinetic sorption data.

Measuring the increase of weight with time, for the samples exposed to the vapour at a given partial pressure, it is possible to obtain the equilibrium value of sorbed vapour, C_{eq} ($\text{g}_{\text{solvent}}/100 \text{ g}_{\text{polymer}}$). Moreover, in the case of Fickian behaviour, that is a linear dependence of sorption on square root of time, it is possible to derive the mean diffusion coefficient from the linear part of the reduced sorption curve, reported as C_t/C_{eq} versus square root of time [25], by the Eq. (1)

$$\frac{C_t}{C_{eq}} = \frac{4}{d} \left(\frac{Dt}{\pi} \right)^{1/2} \quad \text{Eq (1)}$$

where C_t is the penetrant concentration at the time t , C_{eq} is the equilibrium value, d (in cm) is the thickness of the sample and D (cm^2/s) the average diffusion coefficient.

From the first part of the isotherms, when the sorption can be assumed ideal and following the Henry's law, we derived a sorption parameter (S):

$$S = \frac{dC_{eq}}{dp} \quad \text{Eq (2)}$$

where p is the partial pressure of the water vapour.

All the samples showed a Fickian behaviour during the sorption of water vapour at activity $a=0.53$. Using Eq. (1), it was possible to derive the average diffusion coefficient, D (cm^2/s), at every fixed vapour activity ($a= P/P_0$) and the equilibrium concentration of solvent into the sample, C_{eq} ($\text{g}_{\text{solvent}}/100\text{g}_{\text{polymer}}$). The solubility coefficient, S , in cm^3 (STP)/($\text{cm}^3 \cdot \text{atm}$), can be calculated from C_{eq} as follows:

$$S = \frac{C_{\text{eq}}}{100} \frac{\rho}{\text{MW}_{\text{penetrant}}} \frac{22,414}{P} \quad \text{Eq (3)}$$

Where ρ is the sample density, P is the penetrant pressure in atm, $\text{MW}_{\text{penetrant}}$ is the penetrant molecular weight in g/mol, and 22,414 is a conversion factor.

The permeability of the samples to the vapour is given by the product of sorption and diffusion:

$$P = S \cdot D \quad \text{Eq (4)}$$

The gas transport properties were studied for helium and carbon dioxide. The permeation cell consisted in two compartments separated by the studied membrane. The cell was thermostated at $20 \pm 1^\circ\text{C}$. A preliminary high vacuum desorption was realised to ensure that the static vacuum pressure changes in the downstream compartment were smaller than the pressure changes due to the gas diffusion. A 3.0×10^5 Pa gas pressure was introduced in the upstream. The effective membrane area was 3 cm^2 . The pressure variations in the downstream compartment were measured with a datametrics pressure sensor. A steady-state line was obtained after a transitory state by plotting the measured pressure versus time. The permeability coefficient, P , was calculated from the slope of the steady-state line. The diffusion coefficient, D , was deduced from the time lag, θ , provided by the extrapolation of the steady-state line on the time axis.

$$D = \frac{l^2}{6\theta} \quad (1)$$

with l being the thickness of the film.

The permeability coefficient, P , was expressed in barrer unit ($1 \text{ barrer} = 10^{-10} \text{ cm}^3_{\text{STP}} \text{ cm cm}^{-2} \text{ s}^{-1} \text{ cm}_{\text{Hg}}^{-1} = 7.5 \cdot 10^{-18} \text{ Nm}^3 \cdot \text{m} \cdot \text{m}^{-2} \cdot \text{s}^{-1} \cdot \text{Pa}^{-1} = 3.348 \cdot 10^{-16} \text{ mol} \cdot \text{m} \cdot \text{m}^{-2} \cdot \text{s}^{-1} \cdot \text{Pa}^{-1}$), the diffusion

coefficient, D , was given in $\text{cm}^2 \cdot \text{s}^{-1}$. The data were the results of measurements performed on two samples. The precision on P and D values was better than 5%.

3 Results and discussion

3.1 Characterization of organomodified montmorillonites (OMMTs)

3.1.1 Structural analysis by WAXD

The effect of the cationic exchange process on the montmorillonite intercalation was studied by X-Ray diffraction (XRD) and presented in Figure 1.

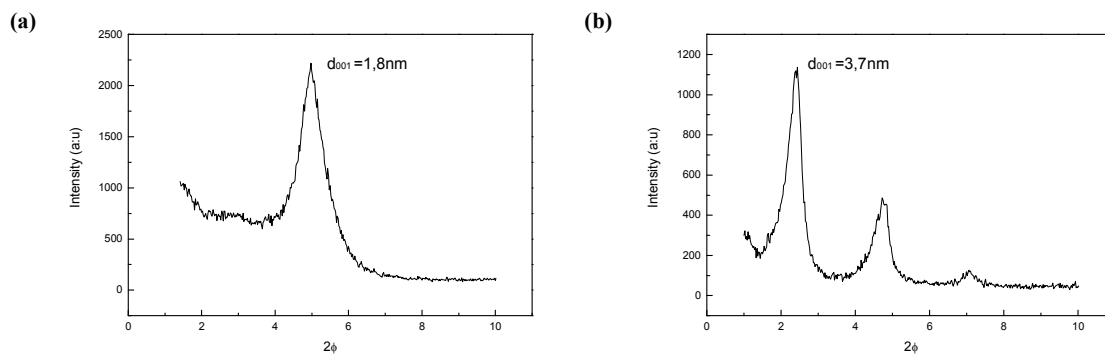


Fig. 1. X-ray diffraction patterns of ionic liquid treated MMT: (a) MMT-201 and (b) MMT-I.

Before organic treatment, the basal spacing of untreated MMT is 1.2 nm, which corresponds to the d-spacing of MMT-Na^+ reported by many authors in the literature [26-27]. After surface treatment with tributyltetradecylphosphonium dodecylbenzenesulfonate (IL 201), the MMT-201 displays a (001) diffraction peak at $5^\circ 2\theta$ corresponding to an interlayer distance of 1.8 nm while the MMT-I displays a diffraction peak at $2.4^\circ 2\theta$ which corresponds to an interlayer distance of 3.7 nm [28]. There are several factors that affect the resulting basal spacing like: i) steric hindrance of ionic liquids and in particular the ii) length of the alkyl chains beared on the phosphonium and imidazolium cations. In fact, in the case of MMT-I,

the value of 3.7 nm could be explained by the presence of two long alkyl chains (C_{18}) and the steric volume occupied by the cation ring. In the opposite, for the MMT-201, the phosphonium cation is only functionalized by three short alkyl chain (C_4) and one long alkyl chain (C_{14}).

3.1.2 Thermal stability of OMMTs

Many authors [29-30] have already identified two kinds of molecular interactions in organically modified clays: (i) Van der Waals bonds between the clay surface and hydrogen from the alkyl chains and (ii) ionic or electrostatic bonds occurring inside the gallery between the surface oxygen of silicon tetrahedral and the protonated cation that varies according to the surfactant agent used (ammonium, pyridinium, phosphonium or imidazolium). Thermogravimetric analysis (TGA) may help to reveal the different mechanisms of degradation of the organic substances on the clay. In fact, different authors have recognized the existence of two separated species present in the thermal degradation of modified- MMT [21, 27]. The first one are physisorbed species, *i.e.* the physically adsorbed species on the clay surface while the second one are intercalated species between the clay layers. Figure 2 displays the evolution of the weight loss as a function of temperature performed on the two montmorillonites exchanged either with imidazolium or phosphonium ionic liquids.

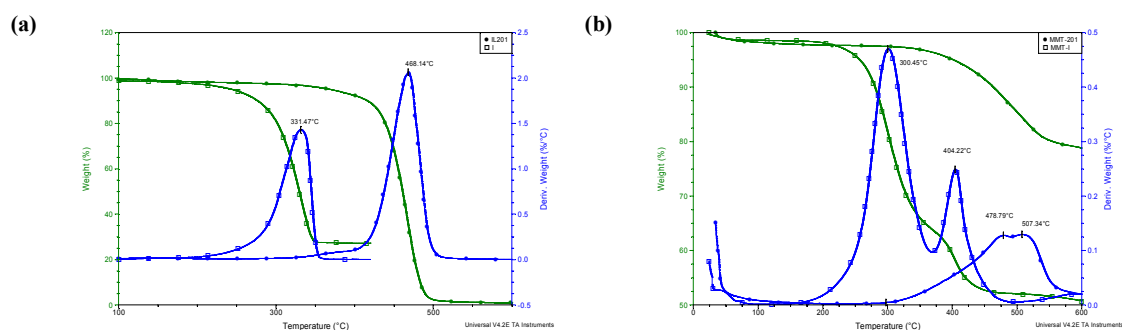


Fig. 2. Evolution of weight loss as a function of temperature (TGA) and derivative of TGA curves (DTG) of the (a) ionic liquids and (b) organically modified montmorillonites. (heating rate 20 °C min⁻¹, under nitrogen flow).

After cationic exchange with phosphonium or imidazolium ionic liquids, two degradation peaks have been identified. In the literature, it has been already reported that the first peak corresponding to the first weight loss highlights the degradation of organic physisorbed species on the clay surface [28]. Thus, on the DTG curves of MMT-I, the degradation of the IL physically adsorbed on the surface starts at 255 °C ($T_{5\%}$), whereas the phosphonium treated montmorillonite (MMT-201) is thermally stable up to 400 °C ($T_{5\%}$). Then, the second weight loss corresponds to intercalation of ILs inside clay galleries. In this case, a difference of 100 °C is observed between MMT-I (405 °C) and MMT-201 (510 °C). These results can be explained by the chemical nature of the ionic liquid and in particular, the intrinsic thermal stability of the cation/anion used. In fact, Awad et al. studied the thermal degradation of montmorillonites modified with different imidazolium based ionic liquids and they found that ILs combined with halides (Cl^- , Br^-) as counter ion presented faster degradation compared to imidazolium ionic liquids with fluorinated anion (BF_4^- , PF_6^-) [13]. Other authors have also studied the different factors responsible for the thermal stability of imidazolium- and phosphonium-modified montmorillonites and they demonstrated that halide salts show the lowest degradation peak [31-32]. However, they have highlighted that phosphonium-treated montmorillonite have greater thermal stability than imidazolium-modified MMT due to the well-known high thermal stability of the phosphore. The results reported in the literature confirm the higher stability of MMT-201 compared to MMT-I. Nevertheless, the thermal behaviour of MMT-I and MMT-201 is significantly better than montmorillonites modified with conventional quaternary ammonium salts [33].

In addition, the amount of physically absorbed and intercalated species was determined from the mass loss percentage in derivative (DTG) curves. The results summarized in Table 2

suggest that imidazolium ionic liquid (IL-I) is introduced more easily between the clay layers compared with IL-201.

Table 2

Relative mass loss percentages of physically absorbed and intercalated species determined by TGA on the treated montmorillonites.

Montmorillonite	%physically absorbed	% ionically intercalated
MMT-201	11	8
MMT-I	34	12

It is important to also emphasize that physisorbed species (34 wt % for MMT-I and 11wt % for MMT-201) could act as compatibilizing agents between the polymer matrix and the layered silicate. Thus, the chemical nature of ionic liquid will play a significant role on the distribution of modified montmorillonites in PBAT matrix.

3.1.3 Surface energy of ionic liquid treated montmorillonites

To reveal the interactions able to be generated by the treated montmorillonites MMT-I and MMT-201 towards the polymeric material as a function of the chemical nature of the ILs, the contact angles and surface energy determined by the sessile drop method on pressed powder are presented in Table 3.

Table 3

Polar and dispersive components of the surface energy on pristine and modified montmorillonites, as well as on the polymer matrix (PBAT), from contact angles with water and diiodomethane (determination on pressed MMT powders).

	Φ water	Φ CH ₂ I ₂	γ Polar (mNm ⁻¹)	γ Dispersive (mNm ⁻¹)	γ Total (mNm ⁻¹)
NaMMT	22.9 + 0.9	33.6 + 0.8	30	43	73
MMT-201	66,1 + 0,4	41,9 + 0,7	9	39	48
MMT-I	92.8 + 0.1	55.5 + 0.6	1	31	32
PBAT	78,6 + 0,2	27,2 + 0,9	3	45	48

According to the literature, poly(butylene adipate-co-terephthalate) is hydrophobic with a surface energy of 48 mN/m while the layered silicates such as MMT are hydrophilic (73

mN/m) [21]. After organic treatment of sodic montmorillonite (Na-MMT) with ionic liquids IL-I and IL-201, an important decrease of the polar component for MMT-I and MMT-201 is observed. In fact, the polar component of the pristine montmorillonite decreases from 30mN/m to 1-3 mN/m for ionic liquid-treated montmorillonites. These results are explained by the presence of long alkyl chains as well as the steric hindrance of the organic salts [21]. Thus, a lower polar component indicates that the hydroxyl groups are well covered by ionic liquid organic chains. These values are consistent with TGA data where MMT-I has greater number of species absorbed on the surface of the MMT. In conclusion, the chemical nature of the ionic liquid (cation and/or anion) but also the amount of physisorbed species plays a key role on the surface energy.

3.2 Characterization of PBAT/modified-montmorillonites nanocomposites

3.2.1 Morphology of nanocomposites

The influence of the chemical nature of the surfactant agents (imidazolium versus phosphonium) on the distribution of layered silicates has been revealed by transmission electronic microscopy (TEM). TEM micrographs are presented in Figure 3.

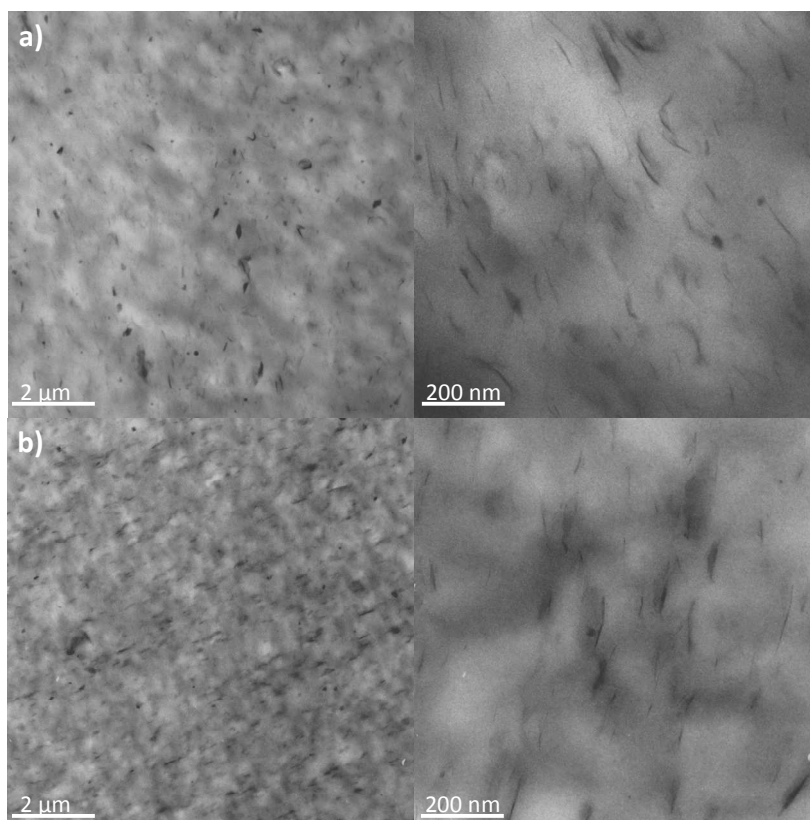


Fig. 3. TEM micrographs of PBAT nanocomposites with 2wt% of OMMT: (a) PBAT/MMT-201 and (b) PBAT/MMT-I

Hence, transmission electron microscopy was used to evaluate the level of dispersion achieved in PBAT nanocomposites filled with 2 wt% of imidazolium- and phosphonium-montmorillonites. Previously, it was shown that the chemical nature of the ionic liquid affected the surface energy of modified montmorillonites. The imidazolium salt led to a less hydrophobic montmorillonite. The final morphology of PBAT nanocomposites processed with imidazolium- and phosphonium-treated montmorillonites significantly depends of the chemical nature of ILs. Thus, a good level of dispersion is obtained with MMT-I compared to MMT-201. The results are similar when 5 wt% of treated MMTs are used. In addition, the presence of ionic liquid physically adsorbed on the montmorillonite surface prevents the use of a large quantity of compatibilizing agent [34-35].

3.2.2 Crystallinity of PBAT nanocomposites

To determine the effect of modified-montmorillonites on the crystallinity of PBAT, differential scanning calorimetry (DSC) was performed on nanocomposites filled with 2 wt% and 5 wt% of PBAT/unmodified MMT, MMT-I and MMT-201. The effect of additional increase of ionic liquid (2 wt%) within nanocomposites was also evaluated. Results are summarized in Table 4.

Table 4: DSC data collected for PBAT and nanocomposites from cooling and second heating scans.

Formulation	T _g (°C)	T _c (°C)	T _m (°C)	ΔH _m (J/g)	X _c %
PBAT	-33	75	122	10,54	9,25
Na+ MMT 2%	-31	72	122	10,11	9,05
Na+ MMT 5%	-32	72	122	10,86	10,03
MMT-201 2%	-32	73	122	10,54	9,43
MMT-201 5%	-34	73	122	10,16	9,38
MMT-201 5% + IL201 2%	-31	76	123	9,77	9,02
MMT-I 2%	-31	72	122	10,47	9,37
MMT-I 5%	-32	73	122	9,9	9,16
MMT-I 5% + IL-I 2%	-30	89	126	5,78	5,34
IL-I 2%	-32	84	125	8,16	9,89

In all cases, the addition of 2 or 5 wt % of montmorillonite modified with phosphonium and imidazolium ionic liquids in PBAT matrix lead to no significant changes in temperature of crystallization (T_c), glass transition (T_g) and melting temperature (T_m) compared to neat PBAT. However, one exception is observed corresponding to the association of the MMT-I with 2 wt % of additional imidazolium ionic liquid. In fact, a significant increase of the T_c is obtained (+14 °C) and this phenomenon is attributed to IL-I incorporation. Generally, increases in T_c suggest the presence of heterogeneous nucleation effect due to clay addition [36-37]. In addition, a good clay distribution within the polymer matrix creates more possible nucleation sites which enhance crystallization of the PBAT nanocomposites. However, this tendency does not apply for PBAT/modified montmorillonites nanocomposites without the

presence of ionic liquid. Despite their good distribution within the polymer matrix, a possible confinement effect imposed by the clay network over the crystal growth might be leading to a slight decrease in the crystallization temperature of nanocomposites [9]. Therefore, we can presume that the addition of ionic liquid to the polymer nanocomposites prevents this constriction effect.

3.2.3 Thermal behaviour of PBAT nanocomposites

The thermal degradation of nanocomposites prepared with imidazolium- and phosphonium-treated montmorillonites nanocomposites are summarized in Table 5.

Table 5

Temperatures at 5% mass loss and peak degradation temperatures of pristine PBAT and nanocomposites (obtained from thermogravimetric analysis).

Formulation	T5% (°C)	Tmax (°C)
PBAT	372	415
MMT-201 2%	371	414
MMT-201 5%	374	416
MMT-201 5% + IL-201 2 %	381	426
MMT-I 2%	369	415
MMT-I 5%	363	417
MMT-I 5% + IL-I 2%	345	421
Na+ MMT 2%	372	416
Na+ MMT 5%	351	407

In the literature, it is well known that the use of nanoparticles, especially layered silicates delays the polymer degradation due to their heat barrier effect [38-40]. Nevertheless, this thermal behaviour is often associated to the morphological structure formed at specific clay loadings (exfoliation and/or intercalation, agglomerates/microcomposites), the chemical nature of the polymer, the type of clay used and their surface treatment [41]. In this work, the addition of 2 wt % and 5 wt% does not improve the maximum degradation temperature of the PBAT nanocomposites. These results can be explained by the small amount of treated montmorillonites introduced in PBAT matrix. In contrast, the combination of imidazolium- and phosphonium-modified montmorillonites with ionic liquid causes an increase in the

thermal stability (+ 10-15 °C) of PBAT which highlights a synergy between the two components. In conclusion, the use of a larger amount of surfactant may contribute to significantly improve the thermal properties of PBAT nanocomposites.

3.2.4 Mechanical properties of PBAT nanocomposites

The uniaxial tensile properties were performed to reveal the impact of 2 wt % and 5 wt % of unmodified and organically modified montmorillonites on the mechanical properties of PBAT. The fracture properties and moduli are detailed in Table 6.

Table 6: Tensile properties of PBAT nanocomposites.

Formulations	Tensile modulus (MPa)	Strain at break (%)	Stress at break (MPa)
PBAT	47 + 1	511 + 17	24 + 1
NA+ MMT 2%	48 + 1	511 + 22	22 + 1
NA+ MMT 5%	56 + 1	470 + 44	20 + 1
MMT-201 2%	50 + 1	514 + 35	21 + 1
MMT-201 5%	55 + 1	452 + 35	21 + 1
MMT-201 5% + IL201 2%	50 + 3	696 + 47	21 + 1
MMT-I 2%	51 + 1	505 + 56	22 + 1
MMT-I 5%	59 + 3	490 + 11	23 + 1
MMT-I 5% + IL-I 2%	69 + 1	749 + 74	23 + 1

The addition of 2 wt % of ionic liquid modified montmorillonites (MMT-I and MMT-201) in PBAT matrix leads to slight increases in the Young modulus (6%-10%) of nanocomposites without reducing the fracture behaviour compared to neat PBAT. The reinforcement effect increases when 5 wt % of MMT-I and MMT-201 is used. In fact, increases in the modulus are in the order of 15-25 % and resulted in a decrease in elongation at break of 10%. However, a synergistic effect occurs when 2 wt % of imidazolium ionic liquid (IL-I) is introduced to PBAT/MMT-I (5 wt %) nanocomposites leading to a significant increase of the tensile modulus (+ 46%) but also improving the strain at break of the polymer matrix (+ 45%). In the opposite, for PBAT/MMT-201 (5 wt %) filled with 2 wt % of IL-201, synergy is clearly less marked with only an increase of the elongation at break. These results are encouraging

compared with those reported in the literature [42-43]. Indeed, Chivrac et al which have investigated the influence of quaternary alkyl ammonium-treated montmorillonite on the mechanical properties of PBAT nanocomposites and they have concluded that the stiffness of the PBAT nanocomposites increased continuously with clay content [42]. Thus, the authors have demonstrated increases on the tensile modulus of 26 % and 47 % (for 3 wt% and 6 wt% of treated MMT used) combined with decreases on elongation at break (10 % and 14 %) and on the stress at break (24 % and 35 %). Other authors have also found the similar results [43]. In conclusion, the imidazolium and phosphonium ionic liquids offer a significant improvement in mechanical properties, especially when the ionic liquid alone is combined with the modified layered silicates.

3.2.5 *Water sorption and permeability of PBAT nanocomposites*

The diffusion of small molecules through polymer nanocomposites is associated with the finite rates at which the polymer structure changes in response to the motion of the permeant molecules and the degree of dispersion of the ionic domains or nanoparticles. Solubility, diffusivity and permeability can be further modified by the presence of organic or inorganic fillers and molecular orientation. Generally, inorganic nanoparticles are used to increase the barrier properties by creating a maze or “tortuous path” that retards the progress of the small molecules through the polymer matrix [44]. The direct benefit of the formation of such a path is clearly observed in all the prepared nanocomposites by dramatically improved barrier properties [45]. Therefore, to determine the influence of the chemical nature of the ionic liquids and their association with montmorillonite on the PBAT matrix, the transport properties were measured for all the samples using water vapour. The water sorption (C_{eq} and S) as well as the diffusion (D) and the permeability (P) of the different PBAT nanocomposites are summarized in table 7 and Figure 4.

Table 7. Water sorption (C_{eq} and S), diffusion (D) and permeability ($P = S \cdot D$) coefficients at activity $a=0.53$ for all the PBAT samples

Samples	C_{eq} (g/100g)	S ($cc_{STP}/cm^3 \cdot atm$)	D (cm^2/sec)	$P((cc_{STP}/cm^3 \cdot atm) \cdot cm^2/sec)$
PBAT	2.37	1.47	$2.26 \cdot 10^{-8}$	$3.32 \cdot 10^{-8}$
PBAT + IL-I (2%)	1.81	1.12	$1.85 \cdot 10^{-8}$	$2.07 \cdot 10^{-8}$
PBAT + MMT-I (5%)	0.58	0.36	$4 \cdot 10^{-8}$	$1.44 \cdot 10^{-8}$
PBAT + MMT-I (5%) + IL-I (2%)	2.47	1.55	$4.30 \cdot 10^{-8}$	$6.66 \cdot 10^{-8}$
PBAT + IL-201(2%)	1.37	0.85	$5.10 \cdot 10^{-8}$	$4.33 \cdot 10^{-8}$
PBAT + MMT-201 (5%)	0.29	0.18	$3.80 \cdot 10^{-8}$	$6.84 \cdot 10^{-9}$
PBAT + MMT-201 (5%) + IL-201 (2%)	0.84	0.52	$4.50 \cdot 10^{-8}$	$2.34 \cdot 10^{-8}$

In all cases, the neat PBAT and the polymer nanocomposites were exposed at a partial pressure of water vapour of 0.53. Thus, the use of ionic liquids IL-I and IL-201 but also the use of 5 wt% phosphonium- and imidazolium-treated montmorillonites MMT-I and MMT-201 leads to a decrease of the water sorption determined either as $C_{eq}(g_{solvent}/100g_{polymer})$ or $S(cc_{STP}/cm^3 \cdot atm)$. Especially, a reduction of water sorption of 75 % and 88 % have been observed for the PBAT nanocomposites containing 5 wt% of MMT-I and MMT-201, respectively. These results can be explained by the hydrophobic nature of the imidazolium and phosphonium salt that are functionalized by long alkyl chains (C_{18} for IL-I and C_{14} for IL-201). According to the literature, compared to the use of ZnO nanoparticles where no change

of the sorption is observed in PLA matrix, the use of ionic liquid modified montmorillonites generates significant decreases [46]. In the opposite, when the addition of ionic liquid is associated with IL-treated montmorillonites, an increase in the sorption is obtained. In fact, the excess of ionic liquid may create channels in the polymer matrix which created a free volume inside the polymer structure allowing easier diffusion of water vapour molecules in PBAT.

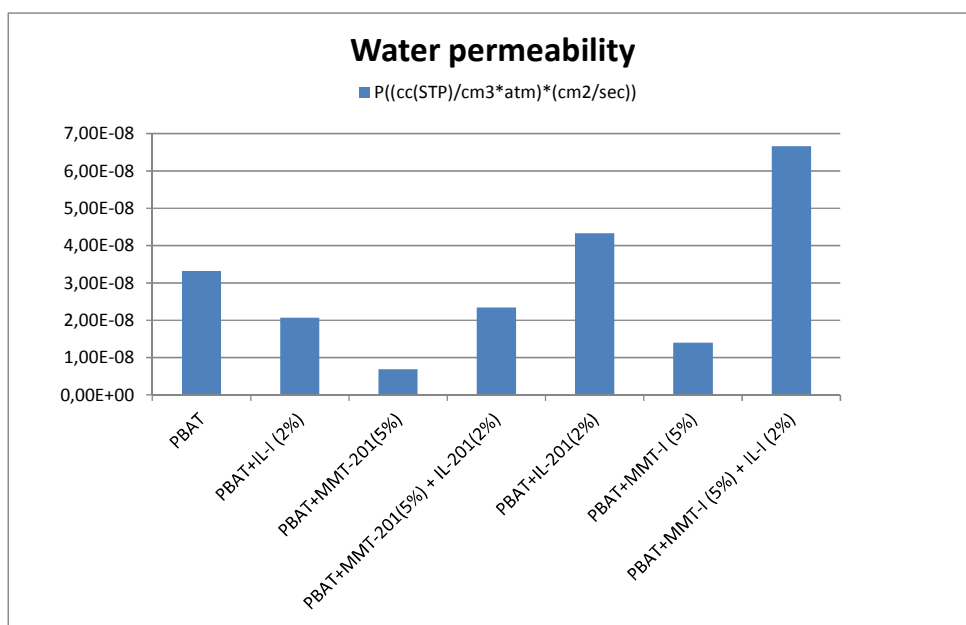


Fig. 4. Water permeability coefficients (P) for all the PBAT nanocomposites

Regarding the water barrier properties of the PBAT nanocomposites, a significant decrease in water permeability is obtained when introducing 5 wt% of ionic liquid modified montmorillonites. In fact, decreases from 60 to 80% are obtained for MMT-I and MMT-201, respectively. These results are promising compared to the results observed in the literature [47-49]. For example, different authors have demonstrated a decrease of only 40% of the vapor water permeability (VWP) when 6 wt% of organically modified montmorillonites were used in PLA matrix [47-48]. Other authors who have investigated the influence of surfactant-

modified cellulose have highlighted decreases in VWP from 5 to 30 % (5% for 5 wt% and 30% for 10 wt% of cellulose) [49]. Finally, many authors have focused on the incorporation of different nanoparticles such as metallic oxides, layered silicates (MMT), layered double hydroxide, or renewable resources such as lignin, cellulose into the polymer matrix with very mixed improvements [50-51]. Other approaches have been investigated with the incorporation of plasticizer such as glycerol or with the combination of renewable sources. Olivato et al demonstrated that the combination of PBAT/glycerol/starch composites induces only a slight decrease of the VWP (7-15 %) depending of the blend composition [50].

In conclusion, the chemical nature of the ionic liquid (cation and counteranion) plays a key role in the water barrier properties. Indeed, the phosphonium ionic liquid functionalized by long alkyl chains and combined with dodecylbenzenesulfonate counteranion (more hydrophobic than iodide) leads to better water barrier properties.

3.2.6 Gas barrier properties of PBAT nanocomposites

Helium and carbon dioxide permeability coefficients are reported in Table 8 for the different films. CO₂ diffusion and solubility coefficients are also presented.

Table 8 He and CO₂ permeability coefficients, P , diffusion coefficients, D , and solubility coefficients, S for the neat PBAT film and the nanocomposites

Sample	P_{He} (barrer)	P_{CO_2} (barrer)	D_{CO_2} ($10^{-8} \text{ cm}^2 \cdot \text{s}^{-1}$)	S_{CO_2} ($10^{-2} \text{ cm}_{\text{STP}}^3 \cdot \text{cm}^{-3} \cdot \text{cm}_{\text{Hg}}^{-1}$)
PBAT	4.56	8.32	4.30	1.93
PBAT/MMT-201 5%	3.40	7.65	3.67	2.08

PBAT/MMT-I 5%	3.56	7.28	3.53	2.06
PBAT/MMT-I 5% + IL-I 2%	3.82	7.78	3.69	2.10

The gas permeability level of the neat PBAT films is rather high and it is noteworthy to remark that the permeability coefficient is almost twofold higher for CO₂ than for He. The small size (2.65Å) and low interaction capacity of He explain its fast diffusion (the time lag is too small to be measured for our films) and the relatively high permeability level. The particularly high value of CO₂ permeability coefficient can be assigned to the major role of the solubility. For this gas, the transitory state is long enough to determine the time lag and as a consequence, the diffusion coefficient. Assuming a Fickian transport, the solubility, S , can be deduced from the P and D values by the following equation:[52]

$$P=DS. \quad (2)$$

S is equal to $1.93 \cdot 10^{-2} \text{ cm}_{\text{STP}}^3 \cdot \text{cm}^{-3} \cdot \text{cm}_{\text{Hg}}^{-1}$. This value is quite important, for example, about threefold the value obtained for polyethylene [52]. However, it is in the same range as that determined for poly(ϵ -caprolactone) [53]. The gas solubility in dense polymer membranes generally results from two contributions: a dissolution phenomenon in unrelaxed holes and interactions between the diffusing molecule and specific polymer sites. The first contribution can be important for glassy polymers. At 20°C, the temperature at which the permeation experiments are performed, the amorphous phase of PBAT is in the rubbery state ($T_g = -33^\circ\text{C}$). The high solubility level determined for this neat polymer can thus be explained, in great part, as for PCL, by the interaction of the polar CO₂ molecule with the ester groups contained in the backbone chains.

Regardless the diffusing molecule, i.e. helium or carbon dioxide, nanocomposites display improved gas barrier properties compared to the reference PBAT film (Table 8).

However, slightly different behaviours are enlightened as a function of the diffusing molecule. Figure 5 represents the relative RP , RD and RS transport parameters, i.e. the ratio between the P , D or S transport parameter for the nanocomposite and the same transport parameter for the neat matrix.

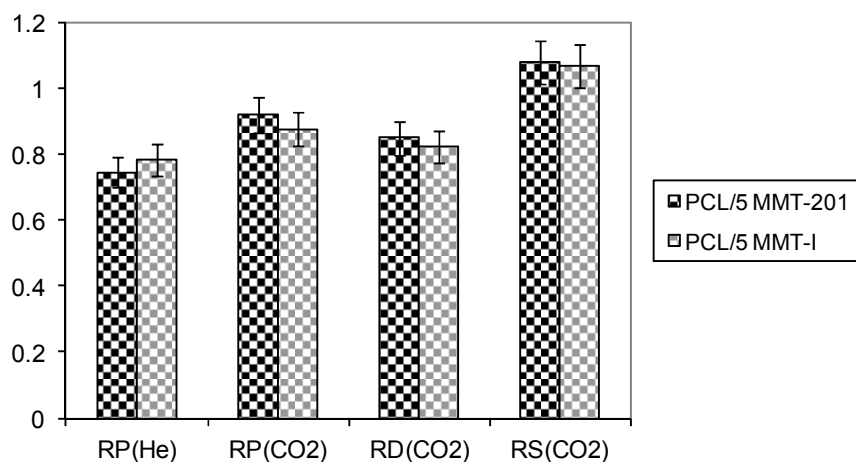


Figure 5: Comparison between the relative permeability (RP), relative diffusion (RD) and relative solubility (RS) values calculated for PBAT/5 MMT-201 and PBAT/5 MMT-I

For PBAT/MMT-201 5% and PBAT/MMT-I 5%, the relative permeability values calculated for He, are slightly lower than 0.8 whereas the values calculated for CO₂ are higher, around 0.9. However, it is noteworthy that the CO₂ relative diffusion values are near to 0.8 whereas the CO₂ relative solubility values are higher than 1. The solubility variation is thus opposite to the evolution predicted by the geometrical approach of the transport phenomenon.[52, 54] Such behaviour has already been observed on different systems and the increase of the solubility coefficient has been related to the presence of tactoids or intercalated structures in which the gas solubility could be favoured. [53, 55, 56] The morphology analysis carried out in our systems has clearly evidenced the presence of intercalated structures dispersed within the matrix. Moreover, the ionic liquid molecules located in the interplatelet space could

provide an enhanced affinity toward CO₂. [57] However, we can observe that the increase of the solubility is in all cases much lower than the decrease of the diffusion coefficient. From this detailed analysis of the gas transport parameters, it can be concluded that a tortuosity effect is at the origin of the enhancement of the gas barrier properties. This tortuosity effect seems to be similar in the PBAT/MMT-201 5% and PBAT/MMT-I 5% nanocomposites. As the crystallinity rate of the matrix is equal to 9.7% in all the considered materials, the tortuosity effect can be assigned to the dispersed nanofillers. According to TEM analysis, the dispersed platelets are perfectly aligned in the plane of the films. Nielsen model can then be used to describe the tortuosity [54]. In this geometrical approach of the gas transport,

$$RP = \frac{(1-\phi_d)}{\tau} = \frac{(1-\phi_d)}{1 + \frac{L}{2w}\phi_d} \quad (3)$$

and

$$RD = \frac{1}{\tau} = \frac{1}{1 + \frac{L}{2w}\phi_d} \quad (4)$$

In these laws, the relative permeability, RP , and the relative diffusion, RD , are a function of the tortuosity, τ , that is related to the length-to-thickness ratio, L/w , and the volume fraction, ϕ_d , of the impermeable dispersed entities. The average length-to-thickness ratio L/w of the dispersed fillers has been determined from the experimental $RP(He)$ values and from the $RD(CO_2)$ values. An average length-to-thickness ratio L/w of the dispersed fillers in the range 16-20 is obtained. This value is consistent with the results derived from TEM observation.

The introduction of a small amount of IL-I in the nanocomposite based on MMT-I, leads to a small increase of all the gas transport parameters, despite a similar dispersion state of the nanofillers (Table 8). The evolution of the gas transport properties can be assigned to the decrease of the matrix crystallinity degree from 9.7% to 5.7% going from PBAT/MMT-I 5% to PBAT/MMT-I 5% + IL-I 2%, and to the increase of the polymer chain mobility induced by the plasticization effect of the ionic liquid. However, it is noteworthy to remark

that the barrier properties of PBAT/MMT-I 5% + IL-I 2% films are still improved in comparison with the neat PBAT films.

4 Conclusion

In this work, phosphonium and imidazolium ionic liquids were used as surfactant agents of layered silicates in order to develop poly(butylene adipate-co-terephthalate) (PBAT) nanocomposites with excellent mechanical and water/gas barrier properties. Thus, the use of thermally stable ionic liquids allows the preparation of polymer nanocomposites at high temperature compared to conventional ammonium salts [33]. Furthermore, the choice of hydrophobic ionic liquids leads to a greater affinity between the layered silicate and the polymer matrix which results in good dispersion of the clay layers in the PBAT. Then, PBAT nanocomposites were prepared by a melt process with only 2 wt% and 5 wt% of imidazolium and phosphonium-treated MMT. As a result, a slight increase in the Young's modulus (15-25 %) without reducing the fracture behaviour is observed. In addition, significant decreases in water barrier properties of the order of 60-80 % as well as for the gas permeation such as CO₂ and helium with decreases of 10-20 % are obtained. The synergy between the ionic liquid and the IL-modified montmorillonites has also been investigated in this study. In fact, the use of the imidazolium salt IL-I generates significant increases in mechanical properties (+ 46 % of Young Modulus and + 45 % of elongation at break) but reduces water and gas properties since the presence of an excess of ILs created channels facilitating the mobility of small molecules. Nevertheless, these preliminary results highlight the true potential of ionic liquids in the preparation of high performance polymeric materials.

References

- [1]M. Okamoto, B. John, *Prog. Polym. Sci.*, 38, 2013, 1487-1503.
- [2]P.X. Ma, *Materials Today*, 7, 2004, 30-40.

- [3]R. Langer, J.P. Vacanti, *Science*, 260, 1993, 920-26.
- [4]P. Törmälä, S. Vainionpää, J. Kilpikari, P. Rokkanen, *Biomaterials*, 8, 1987, 42-45.
- [5]K. Anselme, B. Flautre, P. Hardouin, M. Chanavaz, C. Ustariz, M. Vert, *Biomaterials*, 14, 1993, 44-50.
- [6]R. de Juana, A. Jauregui, E. Calahorra, M. Cortazar, *Polymer*, 37, 1996, 3339-3345.
- [7]E-J. Choi, J-K. Park, *Polymer Degradation and Stability*, 52, 1996, 321-326.
- [8]P. Bordes, E. Pollet, L. Avérous, *Prog. Polym. Sci.*, 34, 2009, 125-155.
- [9]K. Fukushima, M.-H. Wu, S. Bocchini, A. Rasyida, M.-C. Yang, *Materials Science and Engineering: C* 32, 2012, 1331-1351.
- [10]V. Mittal, *Nanocomposites with Biodegradable Polymers: Synthesis, Properties, and Future Perspectives*. Oxford University Press Inc: New York, 2011.
- [11]L. A. d. S. Rodrigues; A. Figueiras; F. Veiga; R. M. de Freitas; L. C. C. Nunes; E. C. da Silva Filho; C. M. da Silva Leite, *Colloids and Surfaces B: Biointerfaces* 103, 2013, 642-651.
- [12]W. Xie; Z. Gao; W.-P. Pan; D. Hunter; A. Singh; R. Vaia, *Chem Mater*, 13, 2001, 2979-2990.
- [13]W.H. Awad, J.W. Gilman, M. Nyden, R.H. Harris, T.E. Sutto, J. Callahan, P.C. Trulove, H.C. Delong, D.M. Fox, *Thermochimica Acta*, 409, 2004, 13.
- [14]J. Zhu, A.B. Morgan, F.J. Lamelas, C.A. Wilkie, *Chem Mater*, 13, 2001, 3774.
- [15]S. Livi, J. Duchet-Rumeau, J-F. Gérard, *European Polymer Journal*, 47, 2011, 1361-1369.
- [16]M.P. Scott, M. Rahman, C.S. Brazel, *European Polymer Journal*, 39, 2003, 1947-1953.
- [17]A.E. Jimenez, M.D. Bermudez, P. Iglesias, *Tribol Int*, 42, 2009, 1744-1751.
- [18]S. Livi, J. Duchet-Rumeau, J-F. Gérard, *Polymer*, 52, 2011, 1523-1531.
- [19]A.A. Silva, S. Livi, D.B. Netto, B.G. Soares, J. Duchet, J-F. Gérard, 54, *Polymer*, 2013, 2123-2129.

- [20] B.G. Soares, S. Livi, J. Duchet-Rumeau, J-F. Gérard, *Polymer*, 53, 2012, 60-66.
- [21] S. Livi, J. Duchet-Rumeau, T.N. Pham, J-F. Gérard, *J. Colloid Interface Sci.*, 354, 2011, 555-562.
- [22] S.Y. Lee, W.J. Cho, K.J. Kim, J.H. Ahn, M. Lee, *J. Colloid Interface Sci.*, 284, 2005, 667.
- [23] R. Herrera, L. Franco, A. Rodriguez-Galan, J. Puiggali, *Journal of Polymer Science : Part A : Polymer Chemistry*, 40, 2002, 4141-4157.
- [24] D.K. Owens, R.C. Wendt, *Journal of Applied Polymer Science*, 13, 1969, 1741-1747.
- [25] W.R. Vieth, M.A. Amini, In: Hopfenberg HB (ed), *Permeability of plastics films and coatings*. Plenum Press, London.
- [26] L. Reinert, K. Batouche, J-M. Lévêque, F. Muller, J-M. Bény, B. Kebabi, L. Duclaux, *Chemical Engineering Journal*, 209, 2012, 13-19.
- [27] S. Livi, J. Duchet-Rumeau, T.N. Pham, J-F. Gérard, *J. Colloid Interface Sci.*, 349, 2010, 424-433.
- [28] S. Livi, J. Duchet-Rumeau, J-F. Gérard, *J. Colloid Interface Sci.*, 369, 2011, 111-116.
- [29] W. Xie, R. Xie, W.P. Pan, D. Hunter, B. Koene, L.S. Tan, R. Vaia, *Chem Mater*, 14, 2002, 4837.
- [30] W. Xie, Z. Gao, W.P. Pan, D. Hunter, A. Singh, R. Vaia, *Thermochim Acta*, 367, 2001, 339.
- [31] C.G. Begg, M.R. Grimmett, P.D. Wethey, *Aust. J. Chem.*, 26, 1973, 2435.
- [32] C. Byrne, T. McNally, *Macromol. Rapid Commun.*, 28, 2007, 780.
- [33] J. W. Gilman; W. H. Awad; R. D. Davis; J. Shields; R. H. Harris; C. Davis; A. B. Morgan; T. E. Sutto; J. Callahan; P. C. Trulove; H. C. DeLong, *Chem Mater*, 14, 2002, 3776-3785.

- [34] S. Boucard, J. Duchet, J-F. Gerard, P. Prele, S. Gonzalez, *Macromol. Symp.*, 194, 2002, 241.
- [35] E. Picard, H. Gauthier, J-F. Gerard, E. Espuche, *J. Colloid Interface Sci.*, 307, 2007, 364.
- [36] F. Yang, Z. Qiu, *Journal of Applied Polymer Science*, 119, 2011, 1426-1434.
- [37] S. Mohanty, S.K. Nayak, *Polymer Composites*, 31, 2010, 1194-1204.
- [38] S. S. Ray, M. Okamoto, *Progress in Polymer Science*, 28, 2003, 1539-1641.
- [39] N.A.I.B.W. Chieng, W.M.Z. Wan Yunus, *Express Polymer Letters*, 4, 2010, 404-414.
- [40] J. Feng; J. Hao; J. Du; R. Yang, *Polymer Degradation and Stability*, 97, 2012, 108-117.
- [41] A. Leszczynska; J. Njuguna; K. Pielichowski; J. R. Banerjee, *Thermochimica Acta*, 453, 2007, 75-96.
- [42] F. Chivrac; Z. Kadlecová; E. Pollet; L. Avérous, *Journal of Polymers and the Environment*, 14, 2006, 393-401.
- [43] Y. Someya; Y. Sugahara; M. Shibata, *Journal of Applied Polymer Science*, 95, 2005, 386-392.
- [44] C. Labruyere, G. Gorrasi, F. Monteverde, M. Alexandre, Ph. Dubois, *Polymer*, 50, 2009, 3626-3637.
- [45] G. Gorrasi, M. Tortora, V. Vittoria, E. Pollet, B. Lepoittevin, M. Alexandre, Ph. Dubois, *Polymer*, 44, 2003, 2271-2279.
- [46] R. Pantani, G. Gorrasi, G. Vigliotta, M. Murariu, Ph. Dubois, *European Polymer Journal*, 49, 2013, 3471-3482.
- [47] C. Thellen, C. Orroth, D. Froio, D. Ziegler, J. Lucciarini, R. Farrell, N. A. Souza, J.A. Ratto, *Polymer*, 46, 2005, 11716-11727.
- [48] Z. Duan, N.L. Thomas, W. Huang, *Journal of Membrane Science*, 445, 2013, 112-118.
- [49] E. Fortunati, M. Peltzer, I. Armentano, L. Torre, A. Jiminez, J.M. Kenny, *Carbohydrate Polymers*, 90, 2012, 948-956.

- [50] J.B. Olivato, M.V.E. Grossmann, F. Yamashita, D. Eiras, L.A. Pessan, *Carbohydrate Polymers*, 2012, 87, 2614.
- [51] D. Mondal, B. Bhowmick, M.M.R. Mollick, D. Maity, N.R. Saha, V. Rangarajan, D. Rana, R. Sen, D. Chattopadhyay, *Journal of Applied Polymer Science*, doi: 10.1002/app.40079.
- [52] M. Barrer, *Diffusion and permeation in heterogeneous media*, in: J.Crank, G.S. Park (Eds.), *Diffusion in Polymers*, Academic Press, New York, NY, 1968, 165-217.
- [53] O. Gain, E. Espuche, E. Pollet, M. Alexandre, Ph. Dubois, *J. Polym. Sci. Part B, Polym. Phys.* 43-2 (2005) 205-214.
- [54] L.E. Nielsen, *J. Macromol. Sci. Chem.* A 1 (1967) 929-942.
- [55] S. Takahashi, H.A. Goldberg, C.A. Feeney, D.P. Karim, M. Farrell, K. O'Leary, D.R. Paul, *Polymer* 47(9) (2006) 3083-3093.
- [56] E. Jacquilot, E. Espuche, J.F. Gérard, J. Duchet, P. Mazabraud, *Journal of Polymer Science, Polymer Physics*, 44 (2006) 431-440.
- [57] P. Li, D.R. T.S. Chung. *Green Chem.*, 14 (2012) 1052-1063.